Analytical and Bioanalytical Chemistry (2019) 411:5149–5157
https://doi.org/10.1007/s00216-019-01892-1

RESEARCH PAPER

Dopamine-functionalized cyclodextrins: modification of reduced graphene oxide based electrodes and sensing of folic acid in human serum

Fereshteh Chekin[1,2] · Vladyslav Mishyn[2] · Alexandre Barras[2] · Joel Lyskawa[3] · Ran Ye[4] · Sorin Melinte[4] · Patrice Woisel[3] · Rabah Boukherroub[2] · Sabine Szunerits[2]

Received: 3 January 2019 / Revised: 26 April 2019 / Accepted: 3 May 2019 / Published online: 27 June 2019

Abstract

A mandatory step in any sensor fabrication is the introduction of analyte-specific recognition elements to the transducer surface. In this study, the possibility to anchor β-cyclodextrin-modified dopamine to a reduced graphene oxide based electrochemical transducer for the sensitive and selective sensing of folic acid is demonstrated. The sensor displays good electrocatalytic activity toward the oxidation of folic acid. The strong affinity of the surface-confined β-cyclodextrin for folic acid, together with favorable electron transfer characteristics, resulted in a sensor with a detection limit of 1 nM for folic acid and a linear response up to 10 μM. Testing of the sensor on serum samples from healthy individuals and patients diagnosed with folic acid deficiency validated the sensing capability.

Keywords β-Cyclodextrin · Reduced graphene oxide · Electrophoretic deposition · Folic acid · Electrochemical sensor

Introduction

Reduced graphene oxide (rGO) has generated great expectations as a transducing platform in electrochemical sensors because of its high electrical conductivity, fast charge transfer kinetics, and the variety of possibilities to integrate an analyte-specific recognition element via simple π-π stacking interactions [1–3]. Next to ligands such as pyrene [4, 5] and tetrathiafulvalene [6, 7], functional dopamine ligands [8, 9] are very attractive. The interest in the use of dopamine is the ease with which functional groups are introduced via the amine terminal group, a strategy that also limits self-polymerization processes at weak alkaline pH. In addition, it was postulated that rGO is likely to oxidize the *ortho*-quinol structure of dopamine to radical or quinone intermediates, which bind covalently to rGO or each other, resulting in functional groups strongly linked to rGO [9].

In this work, we investigate the possibility of anchoring β-cyclodextrin (β-CD)-modified dopamine (dopa-CD) ligands to rGO-based electrochemical transducers. Cyclodextrins (CDs) have been widely used as drug recipients and protein stabilizers [10] because of their hydrophilic shell and hydrophobic cavity, a host for various organic and inorganic guest molecules [11]. Molecules such as dopamine [12–16], ascorbic acid [17], uric acid [14], and tryptophan [18, 19] have been shown to form inclusion complexes with CDs [14, 20–24]. Surprisingly, to the best of our knowledge, this approach has not been considered for the sensing of folic acid (FA). In adults, normal FA blood levels are between 4 and 45 nM [25]. FA is, however, eliminated by the human body, and regular intake is indispensable as deficiency in FA may lead

Electronic supplementary material The online version of this article (https://doi.org/10.1007/s00216-019-01892-1) contains supplementary material, which is available to authorized users.

✉ Fereshteh Chekin
fchekin@yahoo.com

✉ Sabine Szunerits
sabine.szunerits@univ-lille.fr

[1] Department of Chemistry, Ayatollah Amoli Branch, Islamic Azad University, Amol 46178-678, Iran

[2] Université de Lille, CNRS, Centrale Lille, ISEN, Université de Valenciennes, UMR 8520-IEMN, 59000 Lille, France

[3] Unité des Matériaux et Transformations (UMR 8207), Equipe Ingénierie des Systèmes Polymères, Université de Lille, 59655 Villeneuve d'Ascq Cedex, France

[4] Institute of Information and Communication Technologies, Electronics and Applied Mathematics, Université catholique de Louvain, 1348 Louvain-la-Neuve, Belgium

to a number of health problems, such as anemia [26], neural tube defects, and malformation of the fetus during pregnancy [27]. Excess FA in the body can, on the other hand, mask vitamin B_{12} deficiency symptoms [28] and cause other health risks [29].

Although high-performance liquid chromatography (HPLC) remains the routine method for FA quantification [30], the use of electrochemical sensing strategies has attracted considerable attention [31–38] owing to their simplicity and low cost. On most common electrodes, the direct electrochemical oxidation of FA occurs, however, at high overpotentials with sluggish electron transfer kinetics [35, 37]. We demonstrate in this work that modification of rGO/polyethyleneimine electrodes with dopa-CD allows FA sensing in serum at E = 0.68 V versus Ag/AgCl with nanomolar sensitivity.

Experimental

Materials

Potassium hexacyanoferrate(II), folic acd (FA), dopamine, ascorbic acid, uric acid, sodium ascorbate, copper sulfate, dimethylformamide, 1-pyrenecarboxylic acid, acetone, diethyl ether, acetonitrile, dichloromethane, trimethylamine, hydrazine hydrate, hydrochloric acid, magnesium sulfate, triethylamine, polyethyleneimine (PEI; M_w = 25,000), disuccinimidyl carbonate, *O*-(2-aminoethyl)-*O′*-(2-hydroxyl)duodecimethylene glycol, and phosphate buffer tablets were purchased from Sigma-Aldrich. Graphene oxide powder was purchased from Graphenea (Spain). *O*-(2-aminoethyl)poly ethylene glycol modified pyrene (py-PEG) was synthesized as reported earlier by our group [39] and as described in section S1 in the electronic supplementary material.

The characterization methods used are described in section S2 in the electronic supplementary material. Serum samples were provided by CHU Lille with the consent of all participating individual and as approved by the Hospital's Ethics Committee.

Synthesis of dopa-CD

Alkyne-dopamine (300 mg, 1.04 mmol), synthesized according to the method in [40], and β-CD azide (1.08 g, 0.93 mmol), synthesized according to the method in [41], were dissolved in 25 mL of dimethylformamide. $CuSO_4$ (13 mg, 5×10^{-5} mol) and sodium ascorbate (20 mg, 0.1 mmol) were then added, and the mixture was stirred at 80 °C for 24 h under a nitrogen atmosphere. After reaction, the product was precipitated in diethyl ether and washed with acetone. The product, dopa-CD, was purified by column chromatography (SiO_2–acetonitrile/water, 7:3), affording a pale brown solid in 40% yield. ^{1}H NMR (300 MHz, dimethyl sulfoxide), δ (ppm from tetramethylsilane): 8.66 (l, 2H, Ar–OH), 8.08 (s, 1H, triazole), 7.81 (t, 1H, NH) 6.62 (d, 1H, ArH), 6.56 (s, 1H, ArH), 6.42 (d, 1H, ArH), 5.50–5.92 (m, 14H, β-CD OH^2 and OH^3), 4.69–4.95 (m, 7H, β-CD H^1), 4.34–4.64 (m, 6H, β-CD OH^6), 3.99 (t, 2H, O–$C\underline{H}_2$–triazole) 3.49–3.79 (m, 28H, β-CD $H^{3,5,6}$), 3.11–3.47 (m, overlaps with DHO and $C\underline{H}_2$N, β-CD $H^{2,4}$), 2.31 (t, 2H, $C\underline{H}_2$–Ar), 2.09 (t, 4H, $C\underline{H}_2$C=O), 1.74 (quione, 2H, C–$C\underline{H}_2$–C).

Preparation of dopa-CD-modified electrodes

The formation of the dopa-CD-modified electrodes and their functionalization by electrophoretic deposition (EPD) are described in sections S3 and S4 in the electronic supplementary material. The rGO/PEI-coated electrode was immersed for 2 h in an aqueous solution of dopa-CD (120 mM), and then washed twice with water. The interface was further immersed in py-PEG (1 mM) for 2 h to confer antifouling properties to the interface. The interface was finally dried in air and stored at room temperature.

Electrochemical sensing of FA

For the detection of FA, differential pulse voltammograms were recorded in 0.1 M phosphate-buffered saline (pH 7.4) with a modulation amplitude of 5 mV, a step potential of 80 mV, a step height of 15 mV, and a step time of 250 ms. The electrodes were immersed in FA standard solution or in samples (undiluted serum) containing FA for 10 min before analysis. The sensors were regenerated by immersion in NaOH (0.1 M, pH 12.0) for 20 min.

Results and discussion

Formation of β-CD-modified electrical interface

An essential step in any rGO-based sensor technology is the way rGO is transferred onto the electrode. Electrophoretic deposition (EPD) has been shown to be an effective technique for manipulating graphene oxide suspensions with the aim to produce rGO-based films [5, 42, 43]. The capacity of EPD to be used in integrated electrode systems is an advantage over drop casting and other less defined deposition techniques [5, 42, 43]. The concept was developed here on a single gold electrode in an integrated electrochemical system (Fig. 1), as this model system can, later, be easily adapted to an array format. An aqueous solution of graphene oxide/PEI (1:1, ζ = 40.3 ± 2 mV) in a cathodic EPD configuration [4, 5] was used for the local modification of the gold working electrode.

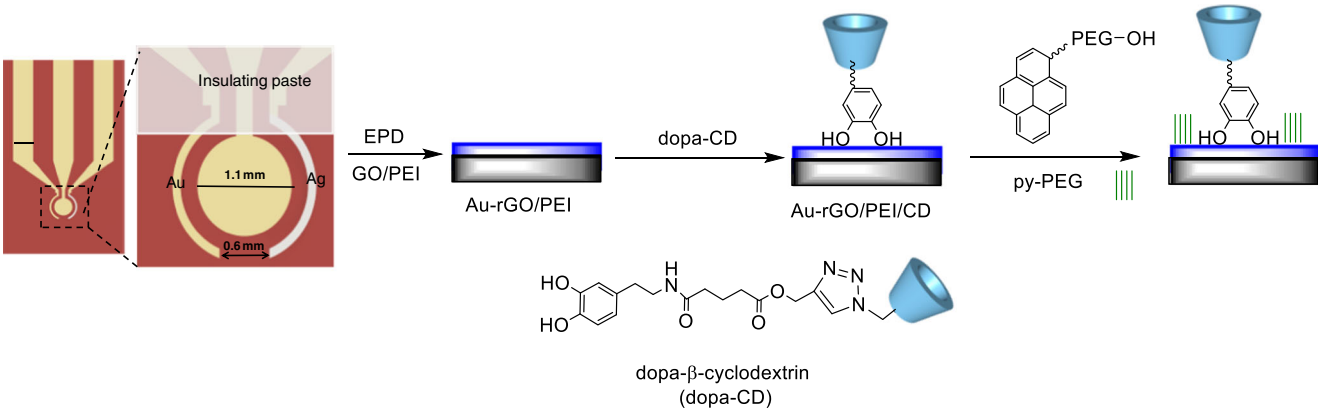

Fig. 1 Modification of an integrated electrochemical system with reduced graphene oxide (rGO) by electrophoretic deposition (EPD) followed by (1) modification with dopamine-modified β-cyclodextrin (dopa-CD) and (2) *O*-(2-aminoethyl)polyethylene glycol modified pyrene (py-PEG). CD: cyclodextrin, GO: graphene oxide, PEI: polyethyleneimine

The photographs of the integrated electrode device before and after modification with rGO/PEI via EPD (Fig. 2a) show initially a smooth morphology, whereas after rGO/PEI coating the working electrode displayed increased roughness. From the scanning electron microscopy image in Fig. 2b and by zooming in on the rGO/PEI-modified part of the electrode, one can observe the formation of an interconnected film of sheetlike structures. The thickness of the deposited layer was about 10 nm, as determined by profilometry measurements. The chemical composition of the formed rGO/PEI film was determined from the X-ray photoelectron spectroscopy (XPS) survey spectrum (Fig. 2c), which comprises peaks at binding energies of 285, 532, and 400 eV, corresponding to C 1*s* (73.80 at%), O 1*s* (14.86 at%), and N 1*s* (11.34 at%), respectively. The C 1*s* spectrum can be deconvoluted into four bands, at 284.6 eV (C–C sp^2), 285.4 eV (C–C sp^3/C–H, C–N), 286.3 eV (C–O), and 287.8 eV (C=O). The high-resolution N 1*s* spectrum (Fig. 2d) reveals the presence of the PEI amine groups (–NH_2 and C–NH–C) at 399.9 and 401.6 eV, respectively.

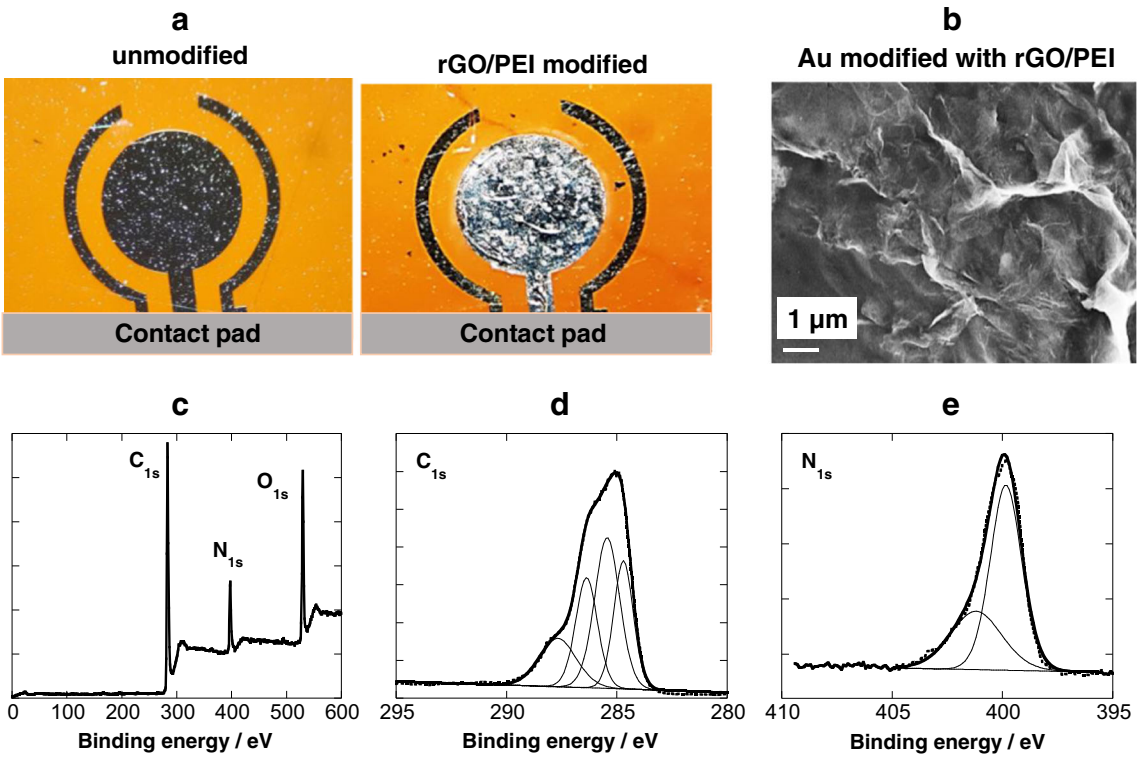

Fig. 2 Characterization of reduced graphene oxide (rGO)/polyethyleneimine (PEI)-modified electrodes: **a** photographs of integrated gold electrodes on a flexible device before and after modification with rGO/PEI; **b** scanning electron microscopy image of the rGO/PEI coating; **c** X-ray photoelectron spectroscopy survey spectrum; **d** C 1*s* spectrum and **e** N 1*s* spectrum of the rGO/PEI-modified electrode

Such electrodes were modified with dopa-CD via π–π stacking interactions between the hexagonal cells of rGO and the aromatic ring structure of dopamine. The success of the surface modification was validated by XPS. The integration of β-CD results in a significant change in the high-resolution C 1*s* XPS spectrum (Fig. 3a), with a strong band at 286.3 eV due to the presence of abundant OH functions of the β-CD ring. In addition, bands at 284.6 eV (sp^2-hybridized carbon), 288.2 eV (C=O, N–C=O, C=N), and 289.7 eV (O–C=O) are observed. The high-resolution N 1*s* spectrum of the CD-modified electrode shows next to the bands of the NH_2 groups of PEI (399.9 eV) components connected to the triazole ring at 402.0 eV (–C-N–) and 401.2 eV (–N=N–), (Fig. 3b). Finally, the interface was immersed in py-PEG (1 mM) for 2 h to provide the interface good antifouling properties [4].

Electrochemical oxidation of FA on Au–rGO/PEI/CD

Characterization of FA/CD complexes in solution indicated that FA could enter the cavity of β-CD spontaneously to form a stable FA–β-CD complex in aqueous solution with a molar ratio of 1:2 (FA to β-CD) and that the pteridine and glutamic acid groups of FA insert themselves into the cavity of β-CD. Figure 4a shows the electrochemical behavior of FA on bare Au and Au–rGO/PEI electrodes. A single well-defined anodic peak appears during cyclic voltammetry with an oxidation peak at $E_{anodic} \approx 0.78$ V on Au in accordance with bare glassy carbon electrodes [34] and at $E_{anodic} \approx 0.71$ V in the case of Au–rGO/PEI. The cathodic potential shift observed on Au–rGO/PEI might be due to prevailing π-π stacking interactions between rGO and the aromatic structures of FA. Integration of dopa-CD onto Au–rGO/PEI shifts the oxidation potential of FA cathodically [14, 23, 44, 45]. The position of the oxidation potential is pH dependent (Fig. 4b) according to E_p (V) = −0.059pH + 1.0303 ($r^2 = 0.9924$). As can be seen from Fig. 4c, the oxidative peak current increases linearly with the scan rate, suggesting that the FA electrochemical oxidation is an adsorption-controlled process [46]. The time of interaction is an important parameter for FA detection. Immersion of the interface for 10 min in FA results in a stable oxidative current (Fig. 4d) and was applied in the following investigations to determine the sensor performance.

Increased current densities are recorded on Au–rGO/PEI/CD electrodes, which was unexpected as the presence of dopa-CD was anticipated to result in partial blocking of the electrode surface by the adsorbed CD molecules [47]. The observed current increase, observed by others as well [14, 23, 44], is probably due to changes in electrostatic interactions between FA, a zwitterion at pH 7.4, and the Au–rGO/PEI electrode.

Sensing of FA on Au–rGO/PEI/CD

To determine whether Au-rGO/PEI/CD is well adapted for sensing FA, differential pulse voltammetry was used (Fig. 5a). The sensor showed a linear range between 5 nM and 10 μM ($r^2 = 0.9998$) (Fig. 5b). The detection limit for FA was determined to be 1 nM from five blank noise signals (95% confidence level) (Fig. 5c) and is comparable with that of iron oxide modified carbon paste electrodes [48] and with that of recently reported MoS_2/rGO thin films [34]. Although other modified interfaces, such as glassy carbon electrode/polymerized thiadiazole films [35], gold/gold nanoparticles–polyoxometalate–polypyrrole [33], or graphene/phosphomolybdic acid–pyrrole [49], show lower detection limits (Table 1), the Au–rGO/PEI/CD sensor can comfortably measure normal and abnormal FA levels (high and low). In healthy adults, the total folate level is between 10 and 30 mg, with blood levels between 4 and 45 nM [25]. Excess FA in the body can, on the other hand, mask vitamin B_{12} deficiency symptoms [28] and can reduce the immune response [29]. The detection limit of the novel FA sensor is comparable to that of HPLC, with the additional advantage of sensor portability, making the device closer to a personalized care sensor.

The FA-sensitive interface, based on rGO/PEI-coated electrodes modified with dopa-CD, is highly stable over time and can be regenerated. This allows prefabrication of the electrodes

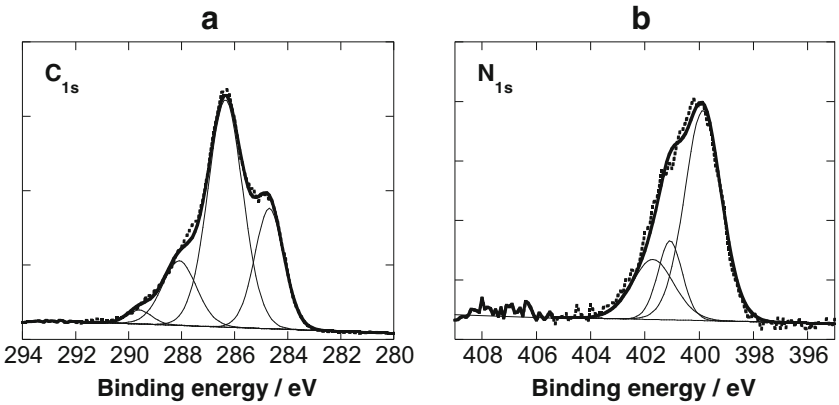

Fig. 3 X-ray photoelectron spectroscopy characterization of the β-cyclodextrin-modified interface (Au–reduced graphene oxide/polyethyleneimine/cyclodextrin): **a** high-resolution C 1*s* spectrum; **b** high-resolution N 1*s* spectrum

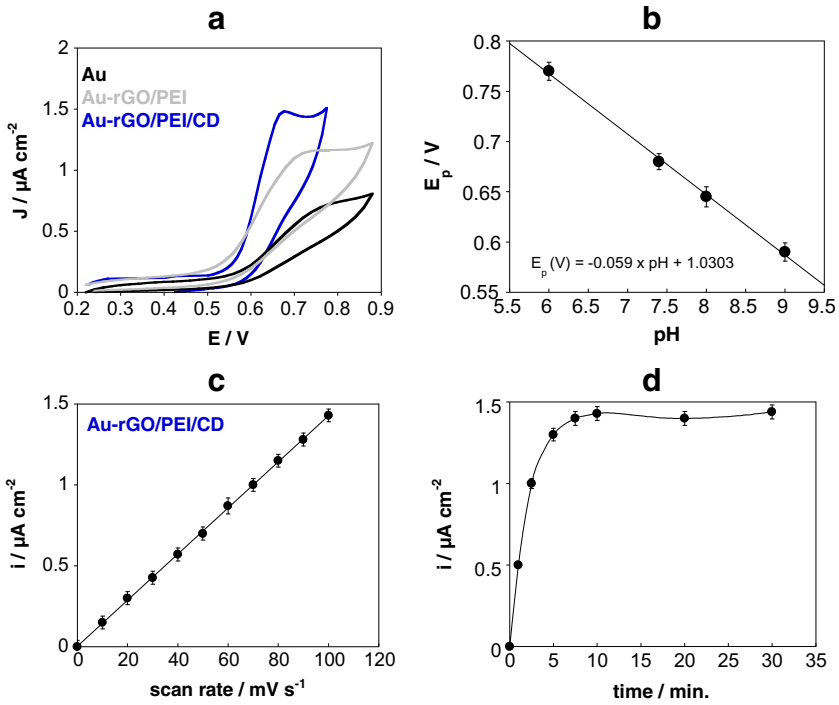

Fig. 4 **a** Cyclic voltammetry response of folic acid (FA; 30 μM) in phosphate-buffered saline (0.1 M, pH 7.4) on Au (gray), Au–reduced graphene oxide (rGO)/polyethyleneimine (PEI) (black), and Au–rGO/PEI/cyclodextrin (CD) (blue); scan rate 100 mV s^{-1}. **b** Change of peak potential with solution pH for FA detection on Au–rGO/PEI/CD. **c** Oxidation peak current versus scan rate for Au–rGO/PEI/CD. **d** Influence of immersion time on oxidative peak current of FA on Au–rGO/PEI/CD

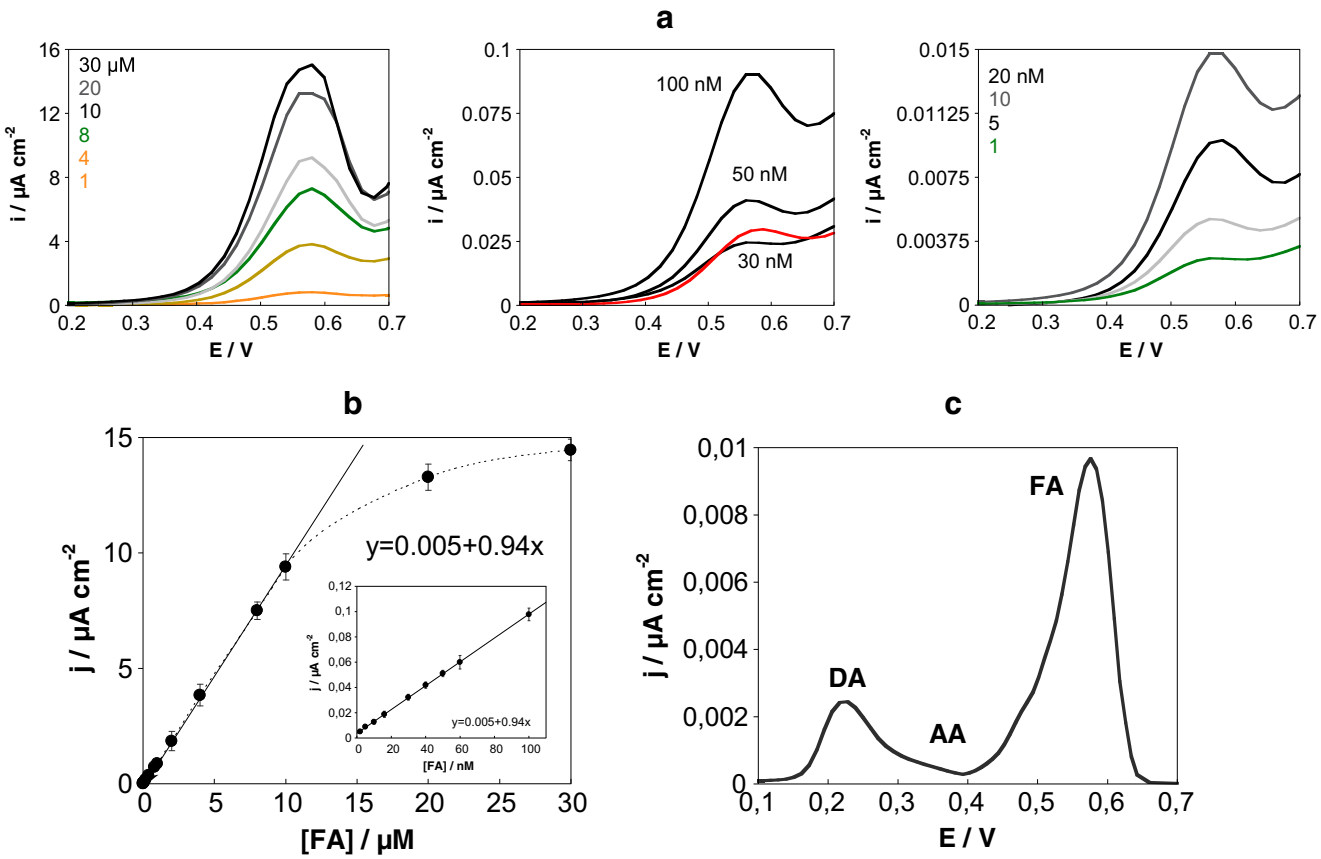

Fig. 5 **a** Differential pulse voltammograms of Au–reduced graphene oxide (rGO)/polyethyleneimine (PEI)/cyclodextrin (CD) in 0.1 M phosphate-buffered saline (pH 7.4) upon addition of folic acid (FA). **b** Change of peak current density as a function of FA concentration; the inset shows an enlargement of the lower-concentration range. **c** Differential pulse voltammogram of the Au-rGO/PEI/CD electrode immersed in a solution of ascorbic acid (AA; 10 nM), dopamine (DA; 10 nM), and FA (10 nM). Error bars indicate the standard deviation of triplicate measurements

Table 1 Characteristics of some electrochemical-based folic acid sensing electrodes

Electrode	Linear range (μM)	LOD (nM)	Reference
ZrO_2 NPs	0.2–2500	9860	[37]
Graphene/MWCNTs	10–170	90	[31]
GCE/Mn–SnO_2 NPs	0.5–900	79	[36]
MoS_2-rGO	0.01–100	10	[34]
Carbon paste electrode/Fe_3O_4 NP modified	0.06–98	2.0	[48]
GCE/polymerized thiadiazole films	0.1–800	0.23	[35]
Gold/Au NPs–polyoxometalate–polypyrrole	0.001–0.04	0.12	[33]
Graphene/phosphomolybdic acid–pyrrole	0.001–0.2	0.03	[49]
Au–rGO/PEI/CD	0.005–10	1.0	This work

CD cyclodextrin, *GCE* glassy carbon electrode, *LOD* limit of detection, *MWCNT* multiwalled carbon nanotube, *NP* nanoparticle, *PEI* polyethyleneimine, *rGO* reduced graphene oxide

and storage before use, making the multistep surface modification protocol of less importance for the final sensing approach.

To evaluate the effect of potential interference by dopamine and ascorbic acid on the sensing performance for FA, the current response of a 10 nM FA solution in the presence of ascorbic acid and dopamine each at the same concentration (10 nM) was recorded (Fig. 5c). Good selectivity toward FA was observed, with a decreased current response for ascorbic acid. This indicates preferential binding of FA to the β-CD cage because of the relatively high complex association constant (K_a = 14.81 × 10^3 M^{-1}) of FA and β-CD [50] as compared with K_a of inclusion complexes between ascorbic acid and β-CD and dopamine and β-CD, with K_a = 3.23 × 10^3 M^{-1} and K_a = 5.88 × 10^3 M^{-1}, respectively [44]. The results also suggest that the main interaction between ascorbic acid may not be inclusion complex formation but rather adsorption, being strongly hindered by the presence of the py-PEG antifouling layer (Fig. 1).

The reproducibility of the sensor for FA sensing expressed in terms of the relative standard deviation was 5.4% at a FA concentration of 10 nM. The sensor also displayed long-term stability when stored at 4 °C for 1 month, with a loss of 4.8% when tested in 10 nM FA. The interface could be regenerated upon immersion in 0.1 M NaOH for 10 min.

Sensing of FA in real samples

A major concern for any electrochemical sensor is related to possible background interferences in real samples. To validate whether the proposed method is suitable for FA detection in biological fluids, the level of FA in human plasma samples was determined by HPLC, a routine method for FA quantification [30], and compared with the differential pulse voltammetry signal obtained with the Au-rGO/PEI/CD sensor. Use of a C_4 HPLC column (5 μm, 250 mm × 4.6 mm) with a mobile phase consisting of a mixture of eluent A (0.05% trifluoroacetic acid in H_2O) and eluent B (0.045% trifluoroacetic acid in CH_3CN) at a flow rate of 1 mL min^{-1} and an isocratic flow (eluent A for 5 min, linear gradient of 0% eluent B to 80% eluent B for 10 min, and further 80% eluent B for 10 min) allowed detection of FA at a retention time of 5 min (Fig. 6a). Under these conditions, a detection limit of 8 nM from five blank noise signals (95% confidence level) (Fig. 6b) was obtained. Both methods were finally used to determine the FA concentration in human serum samples from different donors.

By HPLC, the FA level in serum samples of three healthy individuals was determined to be 32.3 ± 0.8 nM (donor 1), 43.3 ± 0.6 nM (donor 2), and 13.3 ± 0.7 nM (donor 3) (Table 2). The FA levels for these samples determined

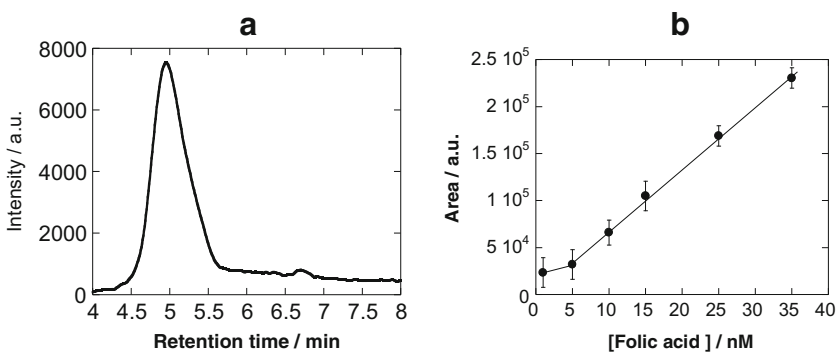

Fig. 6 **a** High-performance liquid chromatography chromatogram of folic acid (35 nM) in acetonitrile/water (2:1) at a flow rate of 1 mL min^{-1}. **b** Calibration curve of folic acid. Error bars indicate the standard deviation of triplicate measurements

Table 2 Folic acid concentrations in human serum of three healthy individuals and three patients determined by the electrochemical sensor and by a high-performance liquid chromatography (HPLC) assay. Error bars indicate the standard deviation of triplicate measurements

Donor	Concentration (nM)		Recovery (%)
	HPLC assay	Electrochemical sensor	
1 (healthy)	32.3 ± 0.8	33.1 ± 0.3	102
2 (healthy)	43.3 ± 0.6	42.3 ± 0.9	98
3 (healthy)	13.3 ± 0.7	12.3 ± 0.5	92
4 (deficient)	12 ± 0.5	15 ± 0.5	125
5 (deficient)	25 ± 0.3	24 ± 0.5	96
6 (deficient)	ND	3 ± 0.5	–

ND not determined

electrochemically were in good agreement with the HPLC analysis. In addition, serum samples from three patients with FA deficiency were analyzed (Table 2). The electrochemical sensor allowed measurement of FA levels of all three patients, even for the donor with a serum concentration as low as 3 nM. Although these data are encouraging and show the potential of the sensor, a larger number of real samples will have to be evaluated to validate further the sensor performance.

Conclusion

In conclusion, we have demonstrated that coupling of of β-CD onto an rGO-based integrated electrochemical system is a promising alternative for FA sensing. The sensor showed FA oxidation at 0.68 V, with improved electron transfer kinetics. Together with preferential formation of a FA/CD complex, selective FA sensing with a detection limit of 1 nM is achieved. The sensor is stable for a long time, with the potential for multianalysis tasks. Testing of the sensor in a limited number of human serum samples from healthy individuals as well as patients diagnosed with FA deficiency validated the sensing capability of the interface. For further application, a pool of patients' samples will have to be tested. Potential interference issues such as unrecorded metabolites/xenobiotics and other species have yet to be studied.

Acknowledgements Financial support from the Centre National de la Recherche Scientifique, the University of Lille, the Hauts-de-France region, the CPER "Photonics for Society," and the Agence Nationale de la Recherche through the FLAG-ERA JTC 2015-Graphtivity project is acknowledged. We are grateful to the Walloon Region for financial support in the frame of the "BATWAL" project - "Programme d'Excellence". Work at UCLouvain has been carried out within the project LUMINOPTEX (avec le soutien du Fonds Européen de Développement Régional / met steun van het Europees Fonds voor Regionale Ontwikkeling - INTERREG V France-Wallonie-Vlaanderen). The work was supported by the Belgian F.R.S. - FNRS in the frame of the research conventions no. R 50.02.16.F and no. T.0106.16.

Compliance with ethical standards

Conflict of interest The authors declare that they have no competing interests.

References

1. Ambrosi A, Chua CK, Latiff NM, Loo AH, Wong CHA, Eng AYS, et al. Graphene and its electrochemistry - an update. Chem Soc Rev. 2016;45:2458–93.
2. Szunerits S, Boukherroub R. Graphene-based bioelectrochemistry and bioelectronics: a concept for the future? Curr Opin Electrochem. 2018;12:141–7.
3. Szunerits S, Boukherroub R. Graphene-based nanomaterials in innovative electrochemistry. Curr Opin Electrochem. 2018;10:24–30.
4. Jijie R, Kahlouche K, Barras A, Bouckaert J, Tijani Gharbi T, Szunerits S, et al. Reduced graphene oxide/polyethylenimine based immunosensor for the selective and sensitive electrochemical detection of uropathogenic Escherichia coli. Sensors Actuators B Chem. 2018;260:255–63.
5. Kahlouche K;R, Jijie IH, Barras A, Gharbi T, Yahiaoui R, Herlem G, et al. Controlled modification of electrochemical microsystems with polyethylenimine/reduced graphene oxide using electrophoretic deposition: sensing of dopamine levels in meat samples. Talanta. 2018;178:432–40.
6. Kaminska I, Barras A, Coffinier Y, Lisowski W, Niedziolka-Jonsson J, Woisel P, et al. Preparation of a responsive carbohydrate-coated biointerface based on graphene/azido-terminated tetrathiafulvalene nanohybrid material. ACS Appl Mater Interfaces. 2012;4:5386.
7. Kaminska I, Das MR, Coffinier Y, Niedziolka-Jonsson J, Woisel P, Opallo M, et al. Preparation of graphene/tetrathiafulvalene nanocomposite switchable surfaces. Chem Commun. 2012;48:1221.
8. Xu LQ, Yang WJ, Neoh K-G, Kang E-T, Fu GD. Dopamine-induced reduction and functionalization of graphene oxide nanosheets. Macromolecules. 2010;48:8336.
9. Kaminska I, Das MR, Coffinier Y, Niedziolka-Jonsson J, Sobczak J, Woisel P, et al. Reduction and functionalization of graphene oxide sheets using biomimetic dopamine derivatives in one step. ACS Appl Mater Interfaces. 2012;4:1016.
10. Szejtli J. Introduction and general overview of cyclodextrin chemistry. Chem Rev. 1998;98:1743–54.
11. Yu G, Jie K, Huang F. Supramolecular amphiphiles based on host-guest molecular recognition motifs. Chem Rev. 2015;115:7240–303.
12. Fritea L, Le Goff A, Putaux J-L, Tertis M, Cristea C, Săndulescu R, et al. Design of a reduced-graphene-oxide composite electrode from an elctropolymerizable graphene aqueous dispersion using a cyclodextrin-pyrrole monomer. Application to dopamine biosensing. Electrochim Acta. 2015;178:108–12.
13. Harley CC, Rooney AD, Breslin CB. The selective detection of dopamine at a polypyrrole film doped with sulfonated β-cyclodextrins. Sensors Actuators B Chem. 2010;150:498–504.
14. Tian X. Simultaneous determination of L-ascorbic acid, dopamine and uric acid with gold nanoparticles-β-cyclodextrin-graphene-modified electrode by square wave voltammetry. Talanta. 2012;93:79–85.

15. Wen D, Liu W, Herrmann A-K, Haubold D, Holzschuh M, Simon F, et al. Simple and sensitive colorimetric detection of dopamine based on assembly of cyclodextrin-modified Au nanoparticles. Small. 2016;12:2439–42.
16. Wu Y, Dou Z, Liu Y, Lv G, Pua T, He X. Dopamine sensor development based on the modification of glassy carbon electrode with β-cyclodextrin-poly(N-isopropylacrylamide). RSC Adv. 2013;3:12726–34.
17. Subhadeep S, Aditi R, Kanak R, Mahendra NR. Study to explore the mechanism to form inclusion complexes of β-cyclodextrin with vitamin molecules. Sci Rep. 2016;6:35764.
18. Liang W, Rong Y, Fan L, Dong W, Dong Q, Yang C, et al. 3D graphene/hydroxypropyl-β-cyclodextrin nanocomposite as an electrochemical chiral sensor for the recognition of tryptophan enantiomers. J Mater Chem C. 2018;6:12822–9.
19. Tao Y, Dai J, Kong Y, Sha Y. Temperature-sensitive electrochemical recognition of tryptophan enantiomers based on β-cyclodextrin self-assembled on poly(l-glutamic acid). Anal Chem. 2014;86:2633–9.
20. Mukdasai S, Poosittisak S, Ngeontae W, Srijaranai S. A highly sensitive electrochemical determination of L-tryptophan in the presence of ascorbic acid and uric acid using in situ addition of tetrabutylammonium bromide on the ß-cyclodextrin incorporated multi-walled carbon nanotubes modified electrode. Sensors Actuators B Chem. 2018;272:518–25.
21. Du D, Wang M, Cai J, Zhang A. Sensitive acetylcholinesterase biosensor based on assembly of β-cyclodextrins onto multiwall carbon nanotubes for detection of organophosphates pesticides. Sensors Actuators B Chem. 2010;146:337–41.
22. Khaled E, Kamel MS, Hassan HN, Haroun AA, Youssef AM, Aboul-Enein HY. Novel multi walled carbon nanotubes/β-cyclodextrin based carbon paste electrode for flow injection potentiometric determination of piroxicam. Talanta. 2012;97:96–102.
23. Alarcon-Angeles G, Pérez-López B, Palomar-Pardave M, Ramírez-Silva MT, Alegret S, Merkoçi A. Enhanced host–guest electrochemical recognition of dopamine using cyclodextrin in the presence of carbon nanotubes. Carbon. 2008;49:898.
24. Tan L, Zhou K-G, Zhang Y-H, Wang H-X, Wang X-D, Guo Y-F, et al. Nanomolar detection of dopamine in the presence of ascorbic acid at β-cyclodextrin/graphene nanocomposite platform. Electrochem Commun. 2010;12:557.
25. Institute of Medicine. Dietary reference intakes for thiamin, riboflavin, niacin, vitamin B_6, folate, vitamin B_{12}, pantothenic acid, biotin, and choline. Washington: National Academies Press; 1988. https://doi.org/10.17226/6015.
26. Ren W, Fang Y, Wang E. A binary functional substrate for enrichment and ultrasensitive SERS spectroscopic detection of folic acid using graphene oxide/Ag nanoparticle hybrids. ACS Nano. 2011;5:6425–33.
27. Breithaupt DE. Determination of folic acid by ion-pair RP-HPLC in vitamin-fortified fruit juices after solid-phase extraction. Food Chem. 2001;74:521–5.
28. Combs GF, McClung JP. The vitamins: fundamental aspects in nutrition and health. San Diego: Academic; 2017.
29. Sanchez H. High levels of circulating folate concentrations are associated with DNA methylation of tumor suppressor and repair genes p16, MLH1, and MGMT in elderly Chileans. Clin Epigenetics. 2017;9:74.
30. Zayed A, Bustami R, Alabsi W, El-Elimat T. Development and validation of a rapid high-performance liquid chromatography–tandem mass spectrometric method for determination of folic acid in human plasma. Pharmaceuticals. 2018;11:52.
31. Abdelwahab AA, Shim YB. Simultaneous determination of ascorbic acid, dopamine, uric acid and folic acid based on activated graphene/MWCNT nanocomposite loaded Au nanoclusters. Sensors Actuators B Chem. 2015;221:659–65.
32. Akbar S, Anwar A, Kanwal Q. Electrochemical determination of folic acid: a short review. Anal Biochem. 2016;510:98–105.
33. Babakhanian A, Kaki S, Ahmadi M, Ehzari H, Pashabadi A. Development of α-polyoxometalate–polypyrrole–Au nanoparticles modified sensor applied for detection of folic acid. Biosens Bioelectron. 2014;60:185–90.
34. Chekin F, Teodorescu F, Coffinier Y, Pan GH, Barras A, Boukherroub R, et al. MoS_2/reduced graphene oxide as active hybrid material for the electrochemical detection of folic acid in human serum. Biosens Bioelectron. 2016;85:807–13.
35. Kalimuthu P, John SA. Selective electrochemical sensor for folic acid at physiological pH using ultrathin electropolymerized film of functionalized thiadiazole modified glassy carbon electrode. Biosens Bioelectron. 2009;24:3575–80.
36. Lavanya N, Fazio E, Neri F, Bonavita A, Leonardi SG, Neri G, et al. Electrochemical sensor for simultaneous determination of ascorbic acid, uric acid and folic acid based on Mn-SnO_2 nanoparticles modified glassy carbon electrode. J Electroanal Chem. 2016;770:23–32.
37. Mazloum-Ardakani M, Beitollahi H, Amini MK, Mirkhalaf F, Abdollahi-Alibeik M. New strategy for simultaneous and selective voltammetric determination of norepinephrine, acetaminophen and folic acid using ZrO_2 nanoparticles-modified carbon paste electrode. Sensors Actuators B Chem. 2010;151:243–9.
38. Prasad BB, Madhuri R, Tiwari MP, Sharma PS. Electrochemical sensor for folic acid based on a hyperbranched molecularly imprinted polymer-immobilized sol–gel-modified pencil graphite electrode. Sensors Actuators B Chem. 2010;146:321–30.
39. Barras A, Szunerits S, Marcon L, Monfilliette-Dupont N, Boukherroub R. Functionalization of diamond nanoparticles using "click" chemistry. Langmuir. 2010;26:13168–72.
40. Kaminska I, Qi W, Barras A, Sobczak J, Niedziolka-Jonsson J, Woisel P, et al. Thiol-yne click reactions on alkynyl-dopamine-modified reduced graphene oxide. Chem Eur J. 2013;19:8673–8.
41. Thorbjørn Terndrup N, Wintgens V, Amiel C, Wimmer R, Lambertsen Larsen K. Facile synthesis of β-cyclodextrin-dextran polymers by "click" chemistry. Biomacromolecules. 2010;11:1710–5.
42. Chavez-Valdez A, Shaffer MSP, Boccaccini AR. Applications of graphene electrophoretic deposition. a review. J Phys Chem B. 2013;117:1502–15.
43. Wang Q, Vasilescu A, Wang Q, Coffinier Y, Li M, Boukherroub R, et al. Electrophoretic approach for the simultaneous deposition and functionalization of reduced graphene oxide nanosheets with diazonium compounds: application for lysozyme sensing in serum. ACS Appl Mater Interfaces. 2017;9:12823–31.
44. Palomar-Pardavé M, Alarcón-Ángeles G, Ramírez-Silva MT, Romero-Romo M, Rojas-Hernández A, Corona-Avendaño S. Electrochemical and spectrophotometric determination of the formation constants of the ascorbic acid-β-cyclodextrin and dopamine-β-cyclodextrin inclusion complexes. J Incl Phenom Macrocycl Chem. 2011;69:91–9.
45. Arvinte A, Marangoci N, Nicolescu A, Pintala M. Electrochemical evidence for inclusion complexes of thiotriazinone with cyclodextrins. RSC Adv. 2016;6:82817.
46. Guzman-Hernandez DS, Palmar-Pardavé M, Rojas-Hernandez A, Corona-Avendano S, Romero-Rom M, Ramirez-Silva MT. Electrochemical quantification of the thermodynamic equilibrium constant of the tenoxicam-β-cyclodextrin inclusion

complex formed on the surface of a poly-β-cyclodextrin-modified carbon past electrode. Electrochim Acta. 2014;140:535–40.
47. Fragoso A, Almill E, Cao R, Echegoyen L, Gonzalez-Jonte R. A supramolecular approach to the selective detection of dopamine in the presence of ascorbate. Chem Commun. 2004;5:2230.
48. Kinesley MP, Desai PB, Srivastava AK. Simultaneous electrocatalytic oxidative determination of ascorbic acid and folic acid using Fe_3O_4 nanoparticles modified carbon paste electrode. J Electroanal Chem. 2015;741:71–9.
49. Wang Z, Han Q, Xia J, Xia L, Bi S, Shi G, et al. A novel phosphomolybdic acid–polypyrrole/graphene composite modified electrode for sensitive determination of folic acid. J Electroanal Chem. 2014;726:107–11.
50. Ceborska M, Zimnicka M, Wszelaka-Rylik M, Tro A. Characterization of folic acid/native cyclodextrins host–guest complexes in solution. J Mol Struct. 2016;1109:114.